PHOTOELECTROCHEMICAL SYSTEMS FOR HYDROGEN PRODUCTION

A. Bansal, Todd Deutsch, Jennifer E. Leisch, Scott Warren and J. A. Turner
National Renewable Energy Laboratory
1617 Cole Boulevard, Golden, Colorado 80401

A.M. Fernández
Departamento de Materiales Solares, CIE-UNAM
Temixco, Morelos, 62580, Mexico.

Abstract

This report summarizes the work from two of the main research areas (surface modification and new materials) that are part of NREL's effort towards a photoelectrochemical-based direct water splitting system. In the area of surface modification for control of bandedge energetics, p-$GaInP_2$ surfaces were modified with pthalocyanins, porphyrins and other organic molecules with the aim of moving band edge positions and catalyzing interfacial charge transfer for photoelectrochemical hydrogen generation. The molecules were adsorbed either by drop coating method or by in-situ deposition. Mott-Schottky measurements in the dark showed that the molecules exhibited varying amount of shifts in the band edge positions. Tetraphenyl porphine Cobalt (II) (CoTPP) showed the largest positive shift (+0.27 V) which is very close to the ~0.3 V shift required to create an unassisted water splitting system. Mott-Schottky measurements of CoTPP modified electrodes under illumination showed that the surface modification led to decreased charge transfer ability and hence greater band edge migration as compared to an unmodified surface. In the area of new materials, ternary semiconductor films based on compositions of Cu-Sb-Se were grown on 304 stainless steel/Cr and ITO-glass using a combination of electrodeposition and chemical bath techniques. The samples were annealed in N_2 atmosphere at various temperatures. Photoelectrochemical studies were used to establish the bandgap, the flat-band potential and the doping density of the material, with an eye towards determining the applicability of the CuSbSe system for the photoelectrochemical decomposition of water.

Introduction

Photoelectrochemical systems being developed for the conversion of solar energy into hydrogen consist of a semiconductor electrode in contact with an aqueous electrolyte. When the semiconductor is irradiated with light greater than its bandgap, photoinduced charge separation occurs in the electrode resulting in a photocurrent in the cell. This photocurrent splits water into hydrogen and oxygen at separate electrode surfaces. For the direct photoelectrochemical decomposition of water to occur, several key criteria of the semiconductor must be met. The semiconductor's band gap must be sufficiently large to split water and yet not too large as to prevent efficient absorption of the solar spectrum (the ideal range then is 1.8-2.2 eV), the band edges of the semiconductor must overlap the hydrogen and oxygen redox potentials, and the charge transfer across the semiconductor/liquid interface must be fast enough to prevent corrosion and band edge migration. Our approach then has been to look for new semiconductor materials with bandgaps in the ideal range and them attempt to catalyze their surface and engineer their bandedges if necessary.

In the area of new materials, we have prepared thin polycrystalline films of Cu-Sb-Se using a combination of electrodeposition and chemical bath technique. X-ray analysis indicates that the films mainly have the Cu_3SbSe_3 phase. The optical and photocurrent measurements show that the band gap is around 1.61-1.68 eV. In this report, we discuss the synthesis and characterization of these films.

Gallium indium phosphide, has a band gap of 1.8-1.9 eV, thus meets the criteria of band gap energy. Its band edges are, however, 0.2-0.4 V too negative to achieve the band edge overlap criteria and they are pH sensitive [1]. The electrode also accumulates photogenerated charges at its surface, thus contributing to surface corrosion and band edge migration away from the desired electrode energetics.

Chemical modifications of the semiconductor electrode surface can help the system ameliorate both these problems. By performing different chemical treatments at the semiconductor surface, the band edges can be shifted to appropriate energetic positions and the interfacial charge-transfer can be catalyzed. We have shown that adsorption of organic and inorganic molecules at p-type $GaInP_2$ can shift the band edges of the semiconductor positive or negative [2]. In particular, we showed that modification of p-$GaInP_2$ surface with 8-quinolinol shifted the semiconductor band edges positive by as much as 0.3 V. On the other hand, we have also shown that transition metals can minimize band edge migration by catalyzing charge transfer across the p-$GaInP_2$/water interface [3].

In this section we combine two surface modification approaches mentioned above by investigating the effects of adsorption of organometallic compounds to simultaneously affect band edge shift as well as act as an electrocatalyst for the p-$GaInP_2$/water interface. Unmetallated and metallated porphyrins as well as pthalocyanins were used in this study to modify the electrochemical properties of the p-$GaInP_2$ electrodes. In addition we also report modifications of p-$GaInP_2$ surfaces with ethylenediammine tetraacetate (EDTA), 3,4,9,10-perylene tetracarboxylic Anhydride (PTCDA) and poly(diallyldimethyl ammonium) chloride (PDDA) as these molecules have also been reported in the literature to affect the band edge positions of

semiconductors. Although pthalocyanins and porphyrins have been widely studied in the literature as photosensitive elements and as catalysts, to the best of our knowledge, this is the first study that explores the effect of these molecules on the photoelectrochemical properties of a semiconductor/liquid junction.

Dark Mott-Schottky Characteristics of p-GaInP$_2$ Surfaces Modified with Porphyrins - Figure 1 shows the flatband potentials of unmodified and porphyrin-modified p-GaInP$_2$ surfaces in pH 7 solution. The solid circles represent surfaces modified by a 'drop-coating' method and the squares represent surfaces modified by an 'in-situ' method. The solid diamond on the left represents the mean value and standard deviation of the flatband potentials measured for an untreated surface in pH 7 buffer solution. The solid black line represents the H_2O/O_2 redox potential. The valence band edge of the semiconductor is ~0.15 V positive of the V_{fb} values shown.

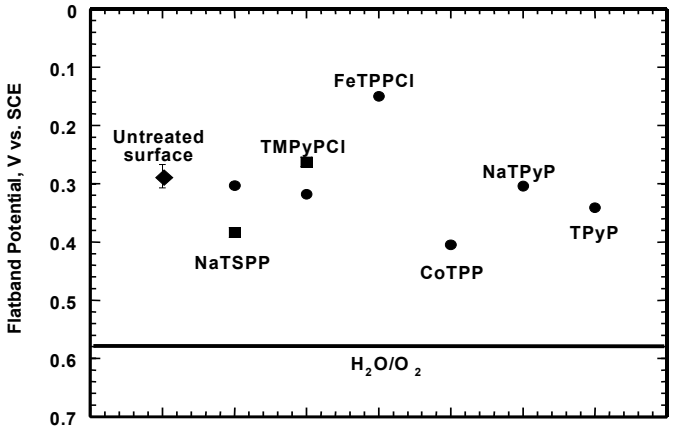

Figure 1: Flatband potentials (V_{fb}) observed for untreated and porphyrin-modified p-GaInP$_2$ surfaces in pH=7 (phosphate) buffer solution. The solid circles represent surfaces modified by the 'drop-coating' method and the squares represent surfaces modified by the 'in-situ' method. The solid diamond represents the mean value of the flatband potentials measured for an untreated surface in pH 7 buffer solution. The error bars represent the standard deviation. The solid black line represents the H_2O/O_2 redox potential. The valence band edge of the semiconductor is ~0.15 V positive of the V_{fb} values shown.

In order for the cell to split water without any external voltage assistance, the measured flatband potential of the semiconductor must be below (more positive of) the H_2O/O_2 redox potential. Figure 1 shows that only three cases show a statistically significant shift in the flatband potential. As compared to an untreated surface in pH 7 solution, the average shift shown by FeTPPCl-treated surface prepared by the drop coating method is –0.14 V, the shift shown by an etched surface run in a pH 7 solution of NaTSPP is +0.10 V and the shift shown by CoTPP-treated surface prepared by the drop coating method is +0.12 V.

Dark Mott-Schottky Characteristics of p-$GaInP_2$ *Surfaces Modified with Pthalocyanins* - Figure 2 shows the flatband potentials of unmodified and pthalocyanin-modified p-$GaInP_2$ surfaces in pH 7 solution. The symbols used here are the same as those used in figure 1. Of all the pthalocyanins used in this study, only two exhibited marginally significant shifts in the flatband potentials. The ZnPc-modified surface prepared by the drop coating method shifted the Vfb by –0.07 V and the etched surface run in $AlPcCl(Sulf)_4$ solution showed a band edge shift of –0.06 V.

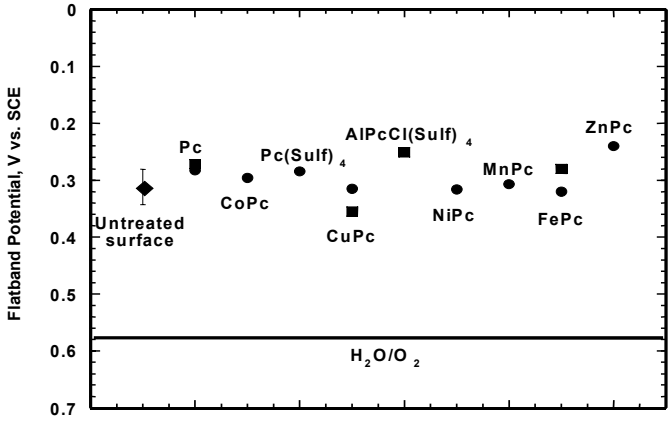

Figure 2: Flatband potentials (V_{fb}) observed for untreated and pthalocyanin-modified p-$GaInP_2$ surfaces in pH=7 (phosphate) buffer solution. The symbols used here are the same as those used in Figure 1. The solid black line represents the H_2O/O_2 redox potential. The valence band edge of the semiconductor is ~0.15 V positive of the V_{fb} values shown.

pH dependence of Flatband Potentials of Modified p-$GaInP_2$ *Surfaces in the Dark* – Figure 3 shows the flatband potential values measured for untreated and modified p-$GaInP_2$ surfaces in solutions of various pH. The only derivatizations that showed statistically significant shifts were Pc tetrasulfonate at pH 0 (-0.09 V), CuPc at pH 0 (-0.09 V), PTCDA at pH 0 (-0.10 V) and CoTPP at pH 4 (0.27 V). Of these, the CoTPP modification in pH 4 solution is of particular interest as the flatband potentials shifted positive by a significant amount and the band edges now overlap the hydrogen and oxygen redox potentials (Figure 3 inset).

Ability of CoTPP to Catalyze Charge Transfer at the p-$GaInP_2$*/Water Interface* – Figure 4 shows the flatband potential values measured for an untreated and a CoTPP-modified surface in pH 4 solution, in the dark and under various levels of illumination. As the level of illumination increases the band edges are observed to migrate negative on both surfaces, indicating accumulation of photogenerated charges at the interface. The Vfb values for CoTPP-modified surface are observed to have shifted more negative than for the untreated surfaces for a corresponding level of photocurrent density.

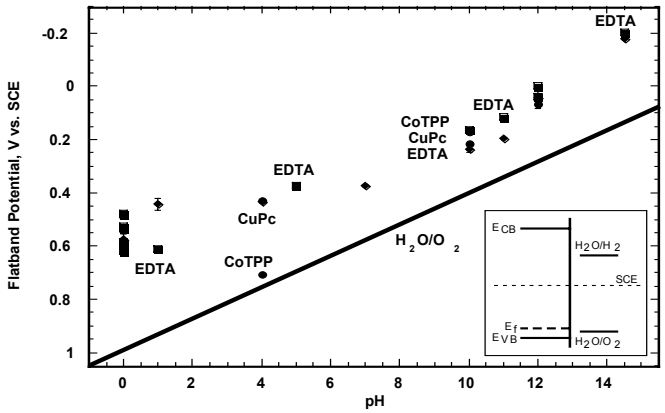

Figure 3: Flatband potentials (V_{fb}) observed for untreated and modified p-$GaInP_2$ surfaces in solutions of various pH. The symbols used here are the same as those used in Figure 1. The solid black line represents the H_2O/O_2 redox potential. The valence band edge of the semiconductor is ~0.15 V positive of the V_{fb} values shown. Inset: Band edge and Fermi level postions of p-$GaInP_2$ with respect to oxygen and hydrogen redox potentials in the liquid phase.

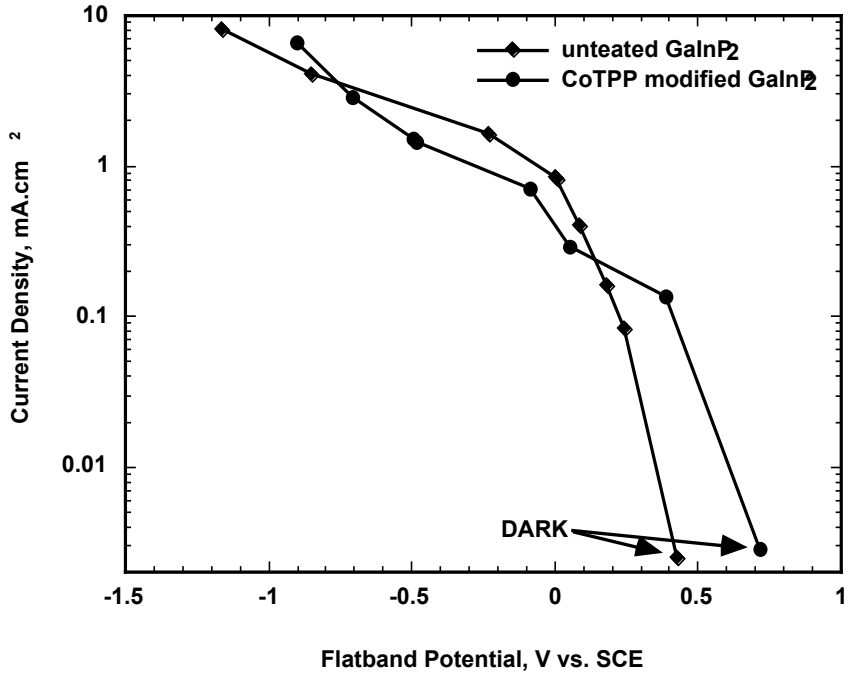

Figure 4: Flatband potentials (V_{fb}) observed for untreated and CoTPP-modified p-$GaInP_2$ surfaces in pH 4 solution, in the dark and under various levels of illumination.

Discussion

Of all the porphyrins, pthalocyanins and other organic molecules evaluated in this study (Figure 3), only a few showed significant band edge shifts. At pH 7, the significant ones were FeTPPCl (–0.14 V), NaTSPP (+0.10 V), CoTPP (+0.12 V), ZnPc (–0.07 V) and $AlPcCl(Sulf)_4$ (–0.06 V). None shifted the band edges positive enough to take it past the water/oxygen redox potential. Measurements made at other pH values also showed shifts of less than 0.10 V, with one exception. p-$GaInP_2$ surfaces modified with drop coated CoTPP exhibited a flatband potential shift of 0.27 V. This was the largest positive flatband shift observed in this study and was significantly within the 0.2-0.4 V range desired for creating a water splitting system.

The CoTPP-treated surface was, therefore, subjected to a more detailed study. It is known that the unmodified p-$GaInP_2$ surface is pH sensitive. To evaluate how the band edges of the modified surface shifted as a function of pH, the CoTPP-treated surface was immersed in solutions of various pH. Figure 5 shows that the CoTPP modified surface is also pH sensitive, albeit to a different extent. It is seen that for pH < 10, the shift in the flatband potential of a CoTPP-modified surface is greater than that for the unmodified surface and this shift increases with decreasing pH. It is advantageous to have a large positive shift as one can expect that part of it would be negated by band edge migration under illumination.

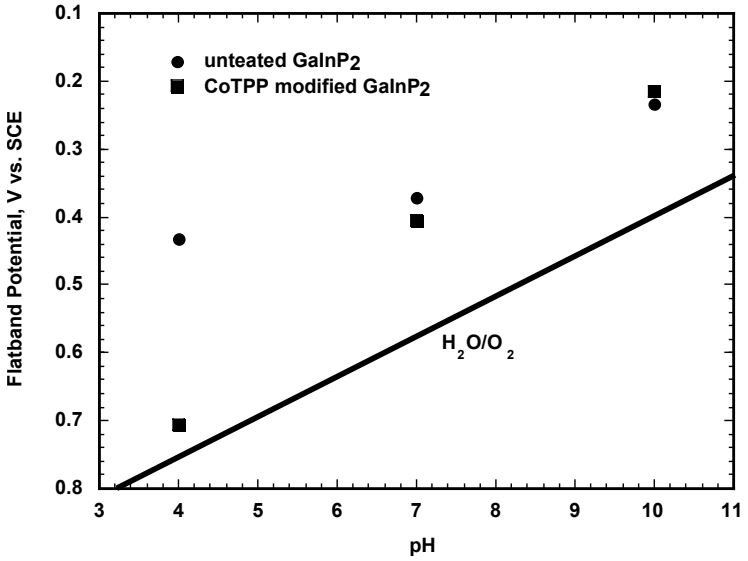

Figure 5: pH sensitivity of band edges for untreated and CoTPP-modified p-$GaInP_2$ surfaces.

Both band edge shift and enhanced charge transfer ability are necessary to realize a viable water splitting system. Therefore, having observed the ability to shift the p-$GaInP_2$ band edges positive, the CoTPP-modified surface was evaluated for enhanced or decreased ability to transfer charge across the p-$GaInP_2$/water interface as compared to the unmodified surface. The migration of the measured flatband potential values towards negative potential in Figure 4 shows that the modified surface continues to have less than optimal interfacial charge transfer rate. When the Vfb values under illumination for both the surfaces are normalized to their respective

Vfb values in the dark, it becomes clear that the CoTPP modification slightly impedes charge transfer. Furthermore, the advantage of positive band edge shift is lost as the illumination level is increased beyond that corresponding to a photocurrent density of approximately 0.2 mA/cm^2 (Figure 4), which is much less than what is required for a working device.

An additional observation from the testing of a variety of organometallic molecules is that the band edge shifting characteristics of a molecule does not depend solely on the organic body of that molecule. Testing of FeTPPCl and CoTPPCl, which have the same organic structure, showed a remarkably different band edge shift characteristics. While FeTPPCl shifted band edge by –0.14 V in the negative direction, CoTPP shifted the band edges positive by +0.12 V. Based on this, it is apparent that the metal ion complexed at the center of the organometallic moiety can play a significant role in determining the extent of the band edge shift

Band Edge Engineering Summary

This section showed that 'band edge engineering' of the p-$GaInP_2$/water interface could be performed by suitable surface treatments of the semiconductor surface. Organometallic molecules such as porphyrins and pthalocyanins can be adsorbed to the semiconductor surface to shift its band edges positive or negative to various extents. The CoTPP-modified p-$GaInP_2$ surface showed a band edge shift of +0.27 V, but the modification reduced the charge transfer efficiency, resulting in increased band edge migration under illumination for the modified surface. It is clear that additional catalysis of charge transfer will be needed to make this system work. Work in this area is currently under progress.

Characterization of Cu-Sb-Se Films Prepared by Chemical-Electrochemical Deposition

Ternary alloy semiconducting materials resulting from alloying of binary semiconducting (having well defined physical properties) usually result in ternary materials whose bandgaps vary between the limits bound by the binary constituents. The three known copper selenoantimonate compounds, $CuSbSe_2$ [4], Cu_3SbSe_3 [5] and Cu_2SbSe_4 [6] have bandgap values between Sb_2Se_3 and Cu_2Se. It is anticipated that, ternary materials resulting from the intermixing of the Sb_2Se_3 with Cu_2Se would have their bandgap varying between 1.55 [7] to 2.2 eV [8], the ideal range for water splitting. Single crystals of the these ternary alloys, which in normal course would be the preference for device applications, may not to be possible over an extended composition range due to the limited solid solubility of Sb_2Se_3 in Cu_2Se. However, the known relaxation of solid solubility limits during thin film growth, coupled with appropriate growth conditions could result in thin films of copper antimony selenide materials.

Considering these aspects, copper antimony selenide films were prepared using a combination electrodeposition and chemical bath technique. In this section, we report on the optical characteristics, the structure, and the atomic composition. Electrochemical measurements in various aqueous electrolyte solutions were done to determinate flat-band potential and photoresponse.

Discussion

The electrodeposition of Sb_2Se_3 is most likely due to the combination of electrochemical and chemical reactions as follows:

	E^o vs. SHE	
$SbO^+ + 2H^+ + 3e^- \longrightarrow Sb + H_2O$	0.212 V	(1)
$H_2SeO_3 + 4H^+ + 4e^- \longrightarrow Se + 3\,H_2O$	0.740 V	(2)
$2Sb + 3Se \longrightarrow Sb_2Se_3$	Chemical reaction	(3)

The mechanism for the formation of the copper selenide has not been established, however, it may be considered as being formed by the following step:

$$2[Cu(NH_3)_4]^{2+} + 2SeSO^{2-}_3 + 4OH^- \longleftrightarrow Cu_2Se + 8NH_3 + 2SO^{2-}_4 + Se + 2H_2O \quad (4)$$

According with the c-T diagram [9] the formation of $CuSbSe_2$ may proceed by the following solid solution reaction:

$$Sb_2Se_3 + Cu_2Se \rightarrow 2CuSbSe_2 \quad (5)$$

Figure 6 shows the growth curve for electrodeposited Sb-Se films and chemically deposited Cu-Se films on 304 stainless steel/Cr substrate. The applied potential is varied for the preparation of the Sb-Se films. In all cases, the Cu-Se films were deposited with the same chemical bath for the same period (six hours). We observed a gradual increase in film thickness with the duration of the Sb-Se film deposition until the film reached the final thickness. Also, it is possible to observe an increment in the rate of deposition when the applied potential increases.

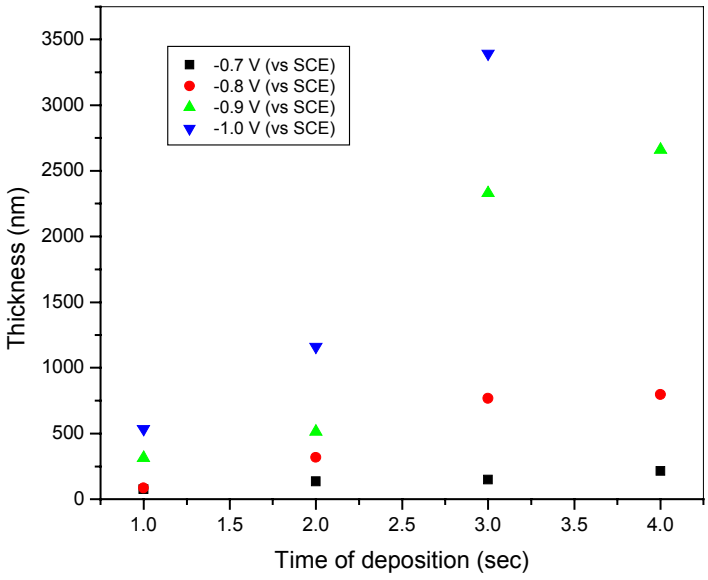

Figure 6: Cu-Sb-Se film thickness as a function of the deposition time of Sb-Se films, at different applied potential of Sb-Se films.

Table 1 lists the atomic ratio of the Cu-Sb-Se films for three different applied potentials. As we observed in the table, after annealing the samples at 400°C, the atomic composition changes drastically, likely due to possible phase changes, from Cu_3SbSe_4 to Cu_3SbSe_3.This effect also shows in the XRD patterns. XRD peaks for annealed samples at 300°C and 400°C in nitrogen atmosphere showed that for the samples annealed at 300°C the major phase corresponded to Cu_3SbSe_4 with a Sb_2Se_3 phase also observed. However, when the samples were annealed at 400°C, the Cu_3SbSe_3 phase was the major phase. This transformation may be possible due to the average Sb-Se distance [8] being almost the same for both compounds as well as the distance between the Cu atoms in the structure.

Table 1: Atomic ratios for three different applied potentials

Sample Number	Applied Potential for Sb-Se electrodep. (V vs. SCE)	Atomic composition Annealed at 300°C			Atomic composition Annealed at 400°C		
		Cu (at.%)	Sb (at.%)	Se (at.%)	Cu (at.%)	Sb (at.%)	Se (at.%)
A	-0.7	35.956	16.106	47.936	45.727	10.060	44.212
B	-0.8	38.811	11.035	50.153	46.353	9.494	44.152
C	-0.9	39.290	13.070	47.639	44.354	12.785	42.859
D	-1.0	33.189	18.174	48.635	44.058	12.949	42.991

The EPMA results for annealed samples of Cu-Sb-Se on 304 stainless steel/Cr substrates. The duration of the time for the deposition of Sb-Se was 45 min., and the duration of time for the deposition of Cu-Se was six hours. The chemical composition for both baths was described above.

The optical transition was be obtained for these films, using the dependence of α on $h\nu$, according to the following relation:

$$\alpha \propto (h\nu - E_g)^n \qquad (6)$$

where α is the absorbance, ν the frequency of wavelength, h the Planck constant and E_g the optical bandgap. Table 2 shows the variation of the bandgap after annealing at 300°C and 400°C.

Table 2: Variation of the bandgap after annealing

Sample number	Optical Bandgap E_g (eV) Annealed temperature, in N_2 atmosphere	
	300°C	400°C
A	1.85	1.58
B	1.78	1.70
C	1.83	1.67
D	1.80	1.65

The bangap values (E_g) for annealed samples of Cu-Sb-Se on ITO-glass. The experimental conditions for the preparation of the samples were described above.

The current-voltage curves showed a low cathodic current density below open-circuit voltage down to about –1.0 V, indicating that the samples are p-type. When the samples were exposed to the light the reverse current increased as expected.

Figure 7 shows a typical Mott-Schottky (M-S) plot ($1/C^2$ *vs*V) for sample D (see Table 1). The plot is fairly linear. Very little hysteresis was seen in all of the samples tested. The slope of the linear portion was slightly frequency-dependent, and showed no variation with pH. Inserting the value of this slope into the Mott-Schottky relationship:

$$\Delta(C^{-2})/\Delta V = 8\pi/\varepsilon q N_D$$

where the ε is the dielectric constant of the semiconductor, N_D is the donor density and q is the absolute value of the elemental charge, a value of $N_D \cong 1.1 \times 10^{20}$ cm^{-3} was found. The intersections of the extrapolated linear portion with V-axis give the flat-band potential. The following values were found: V_{fp} = 0.622, -0.5071, -0.3765, and –0.2773 V at pH = 3,5,7 and 10, respectively. The results demonstrate that the flat-band potential V_{fp} shifts towards positive voltages with increasing pH. The variation of V_{fp} versus pH, yielding a straight line with a slope of 0.0528 V per pH unit.

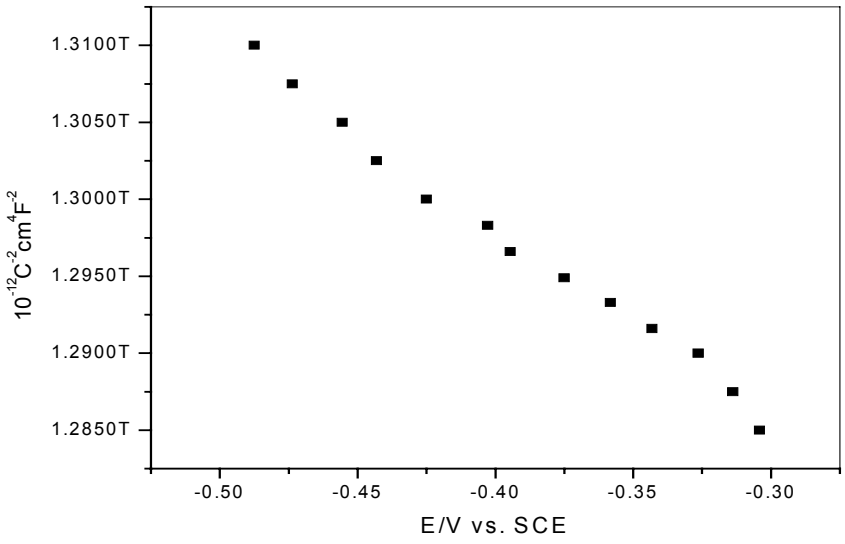

Figure 7: Mott-Schottky plot (*f* = 10 kHz) for Cu_3SbSe_3 in aqueous electrolyte of pH 3.

Figure 8 shows a plot of photocurrent versus wavelength for a sample D under reverse bias. By plotting a function of the current versus the energy of incident light, and extrapolating to zero, the direct band gap was found to about 1.61 eV. This value is very close to the previous value obtained by optical measurement.

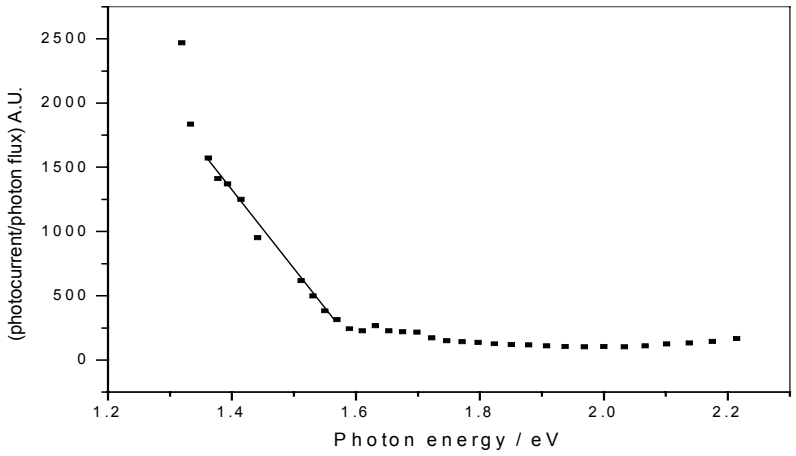

Figure 8: Band gap analysis of Cu_3SbSe_3 for direct (I^2) gap. The graph shows that the bandgap is 1.61eV.

New Material Summary

We reported the preparation of Cu-Sb-Se films using a combined electrodeposition and chemical bath technique. After annealing, the films were polycrystalline with expected atomic composition. The EPMA and XRD analysis indicated that the films mainly have the Cu_3SbSe_3 phase. The optical and photocurrent measurements show that the band gap is around 1.61-1.68 eV. The flat-band potential values and a doping density of about 1.1 x 10^{20} cm^{-3} were observed. The shift in the flat-band potential with the pH is linear, with slope of about 53 mV per unit pH. This material will now be studied for possible water splitting activity.

Acknowledgements

We thank Dr. Brian A. Gregg of NREL for providing us the various pthalocyanins, porphyrins, PTCDA and PDDA. SW, JL and TD thank Linda Lung and acknowledge funding from the summer ERULF program.

This work was supported by the Hydrogen Program of the U.S. Department of Energy.

References

1. S. S. Kocha, J. A. Turner, and A. J. Nozik, *J. Electroanal. Chem.* **1994**, *367*, 27.
2. S. Kocha, J. A. Turner, *Journal of The Electrochemical Society*, **142**, 2625, (1995)
3. A. Bansal, and J. A. Turner, *J. Phys. Chem. B*, 104, p 6591, (2000).

4. R.M. Imamov, Z.G. Pinsker, and A.I. Ivchenko. *Soviet Phyiscs-Crystallography,* **9** (1965) 721.
5. A. Pfitzner, *Z. anorg. Allg. Chem.,* **621** (1995) 685.
6. A. Pfitzner, *Zeitschrift für Kristallographie,* **209** (1994) 685.
7. A.P. Torane, K.Y. Rajpure, C.H. Bhosale, *Materials Chemistry and Physics,* **61** (1999) 219.
8. V.M. García, P.K. Nair, M.T.S. Nair, *Journal of Crystal Growth,* **203** (1999) 113.
9. G.B. Gather, R. Blachnik, *Journal of the Less-Common Metals,* **48**(1976) 205
10. J. Li, Z. Chen, R-J Wang, D.M. Proserpio, *Coodination Chemistry Reviews,* 190-192 (1999) 707.